



Geocells for Transportation Geotechnical Applications

Gali Madhavi Latha¹

Received: 13 November 2020 / Accepted: 23 April 2021 / Published online: 19 May 2021
© Indian Geotechnical Society 2021

Abstract Since their inception in early 70s, geocells have found numerous applications in civil engineering. One of the most important applications of geocells, which has created considerable impact in the field of reinforced soil structures, is their usage in various transportation geotechnical applications. Geocells are successfully being used for the reinforcement of road embankments, unpaved roads and creation of flexible retaining walls. This paper demonstrates the beneficial effects of geocells in all these applications through laboratory model studies. Embankments were built on soft clay with the support of a geocell layer, withstanding higher loads with lesser settlements. Geocell reinforcement in unpaved roads has significantly improved the cyclic load-bearing capacity and resilient modulus, improving the traffic benefit ratio and reducing the rutting. Geocell walls built with low-cost polymers could sustain severe earthquake conditions, without undergoing failure.

Keywords Geocell · Embankments · Unpaved roads · Retaining walls · Reinforced soil

Introduction

The primary application of Geocells, when they were conceptualized and implemented in 1970, was providing immediate support for the movement of heavy military vehicles over soft roads [1, 2]. Over the years, geocells

have found many other applications like foundation reinforcement, erosion control, slope protection, channel protection, flood walls and blast protection. However, the use of geocells in various transportation-related applications, including roads, embankments and retaining walls, remains well ahead among all other applications. Today, geocells are being extensively used across the world, to construct low maintenance roads in difficult ground conditions. Many case studies are available in literature, demonstrating the successful performance of geocells in protecting the roads and other components of transportation infrastructure against adverse weather conditions, earthquakes and floods.

Pokharel et al. [3] discussed the field size pilot studies on geocell reinforced unpaved road sections built in Northern Alberta and British Columbia. These roads are geographically located in places prone to cold winters and extreme freeze and thaw conditions. An excellent case study of building a geocell flood wall in a short time to protect the city of Smithland, Kentucky from flood was reported by Geocell Systems Inc. [4]. Another case study of a 15 m tall geocell retaining wall built in Istanbul to resist seismic loads was illustrated by PRS Geotechnologies [5]. The geocells were made of low tensile strength uniaxial geogrids but provided high strength, flexibility and resistance to extreme earthquake motions. Another case study of rehabilitation of damaged roads due to heavy rainfall in Hangal of North Karnataka using geocells is documented by Bagli [6]. Geocells provided a long-term solution to the problems of reflective cracking, rutting and mud-pumping, which were a constant hurdle to the movement of vehicles during every monsoon season.

Several earlier researchers have presented the beneficial effects of geocell reinforcement for transportation applications through laboratory model tests. The beam effect and all-round confinement effect of geocells were

✉ Gali Madhavi Latha
madhavi@iisc.ac.in

¹ Department of Civil Engineering, Indian Institute of Science, Bangalore 560 012, India

conceptually explained by Han et al. [7]. Bathurst and Karpurapu [8] and Rajagopal et al. [9] quantified the all-round confinement effect of geocells through large-scale laboratory triaxial tests. Krishnaswamy et al. [10] showed that geocell confinement can drastically reduce the vertical settlements and heave of embankments built on soft clay layers. Benefits of geocell reinforcement in reducing cyclic deformations in soils were investigated by Latha et al. [11], Nair and Latha [12] and Latha and Manju [13]. Thakur et al. [14] showed that the all-round confinement effect of geocells is capable of reducing creep deformations in recycled asphalt pavements. Leshchinsky [15] presented results from simulated load tests on models of railroad ballast embankments, showing that geocells are effective in controlling the permanent deformations and degradation of ballast to slow down the deterioration of the embankment geometry under heavy-duty rail traffic movement. Saride and Rayabarapu [16] discussed different methods of design of pavements reinforced with geocells, in the light of laboratory model pavement studies on geocell reinforced granular bases.

This paper presents some important laboratory and small-scale field simulations on geocell reinforced embankments, road sections and retaining walls.

Geocell Supported Embankments

Embankments to support road and rail-road traffic movement are essential components of transportation network. In countries like India, where diverse soil conditions pose many challenges for the construction and maintenance of these embankments, supporting these embankments on a strong geo-cellular network is a sustainable solution. Since geocells are tri-planar, they confine the infill soil in both lateral and vertical directions, thus providing a strong mat-like foundation to the embankment. Apart from transferring their tensile stiffness to load-bearing capacity of soils, geocells also contain the soils, allowing for the re-orientation of shear planes and reducing the load on the foundation soil. The pressure bulb, which usually extends to deeper soils, is widened and limits itself to shallow depths of the soil layers due to the beam effect of geocells, thus allowing constructions on weaker soils. Most importantly, the benefits of geocell are immediate and hence the disturbance to traffic movement during the construction phase is minimal. Additional supporting system for compactors and trucks carrying construction materials are also not needed since geocells provide full-support for the vehicular traffic, as soon as they are expanded in the field and filled with the infill material. Figure 1 illustrates a geocell supported embankment constructed over a soft clay foundation bed.

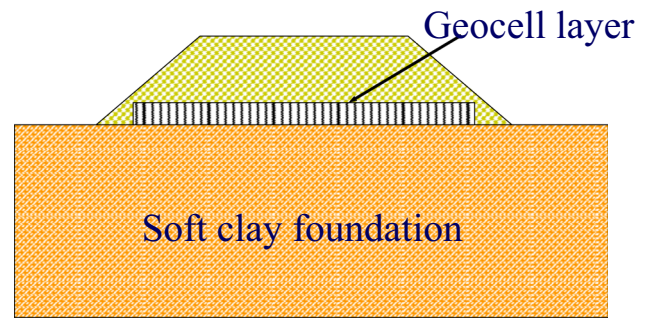


Fig. 1 Schematic diagram of a geocell-supported embankment

To understand the benefits of geocell reinforcement in embankments over soft soil beds, laboratory plate load tests were carried out. A soft clay bed of 0.4 m depth was created by mixing a lot of water with clay and consolidating it for a week by applying a uniform surcharge of 10 kPa. At the end, the shear strength and CBR properties of the clay bed were measured by taking undisturbed samples from the prepared test bed. The unit weight of the test bed was 17 kN/m^3 , CBR value in soaked condition was 0.5% and the undrained cohesion was 20 kPa. Uniaxial and biaxial geogrids and geonets were used in different model tests to fabricate the tri-planar honeycomb-shaped geocells. Table 1 presents the properties of these geosynthetics. Clayey sand was filled in geocells and carefully compacted to a unit weight of 17 kN/m^3 . The aperture openings of all geogrids and geonets are at least 20 times larger than the average particle size of the clayey sand, allowing free passage of clayey sand between the interconnected cells through the openings. In readymade geocells where polymeric sheets are ultrasonically welded, such soil movement is restricted, imposing additional confining pressure inside the cells.

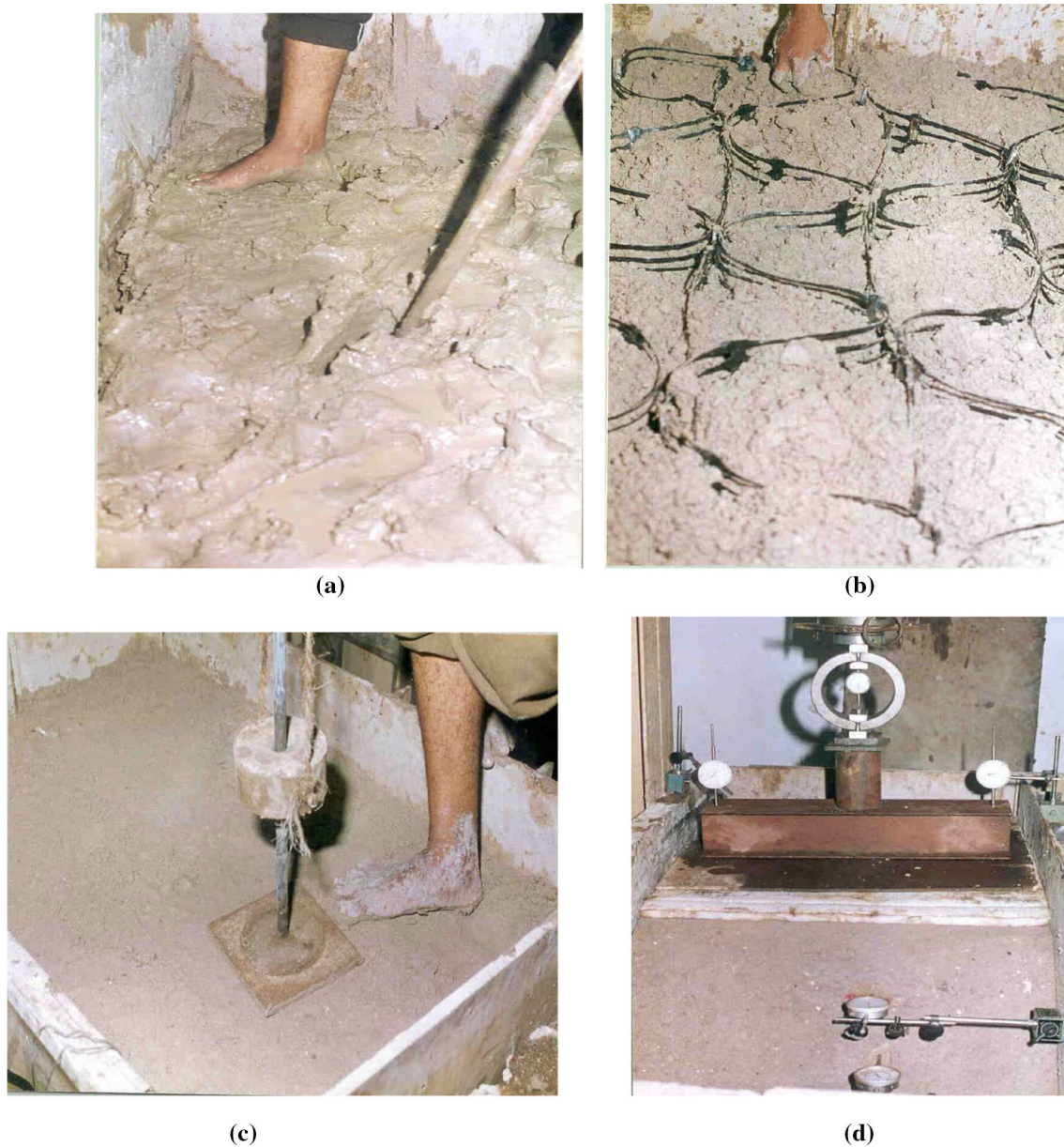
Symmetric half models of soil embankments of base length 1.8 m, width 0.8 m and height

0.6 m were built on top of the geocell layer using clayey sand to a unit weight of 19 kN/m^3 . Plate load tests were conducted on the model embankments and settlements of the embankment, deformations of the slope and heave of the soil layer adjacent to the embankment were measured using dial gauges. Figure 2 shows the sequence of the model construction and testing.

Results from the load tests on model embankments proved that geocells provided at the base of the embankment are effective in controlling the vertical and lateral deformations of the embankment. Variation of vertical deformations with different aspect ratios of geocell layer created using single-plane biaxial geogrid is shown in Fig. 3. The position of dial gauges is marked with V in Fig. 3. As seen from the figure, inclusion of the geocell layer has significantly reduced the settlements of the

Table 1 Properties of geosynthetics used for making geocells in model tests

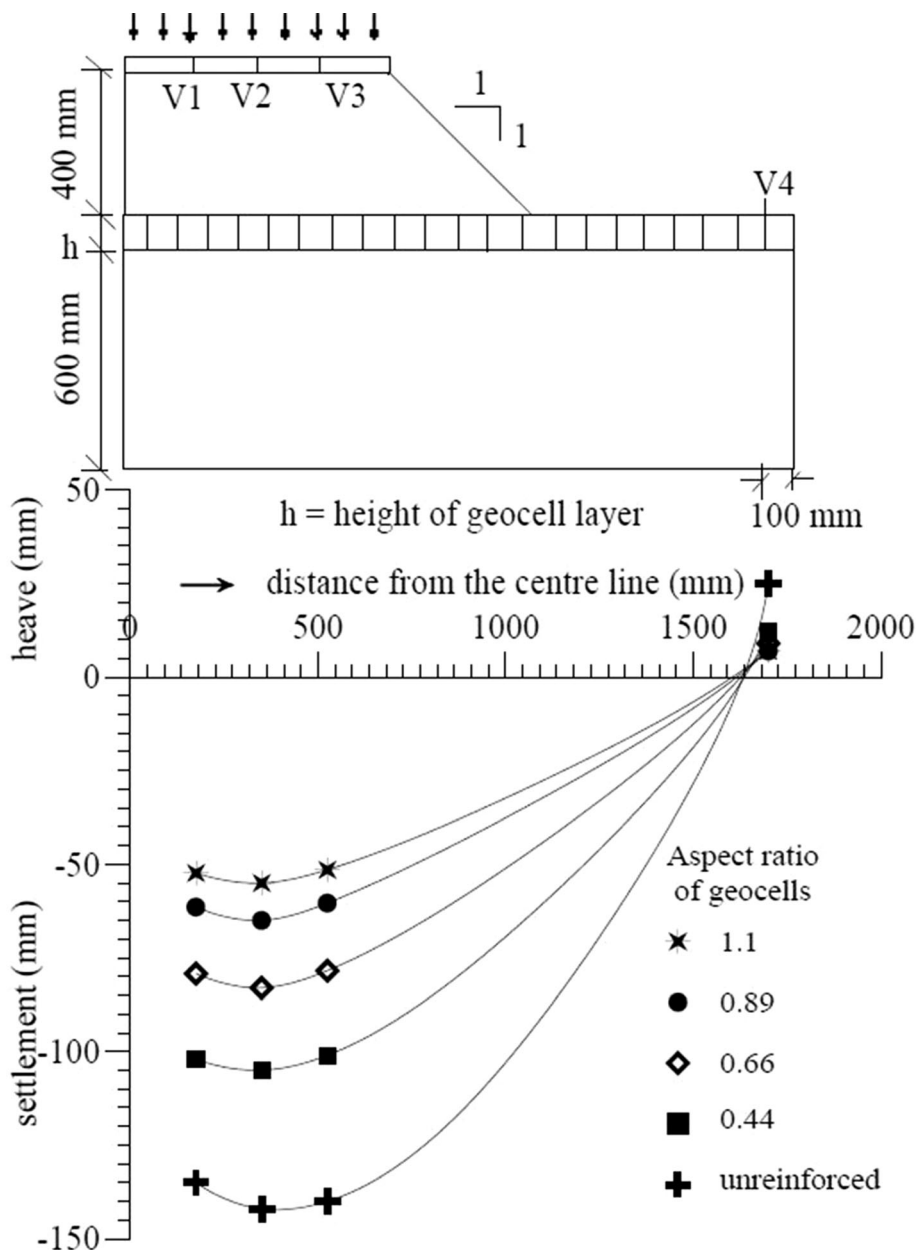
Property of geosynthetic material	Uniaxial geogrid	Biaxial geogrid	Geonet
Ultimate tensile strength (kN/m)	40	20	4.5
Failure strain (%)	28	25	10
Aperture opening (mm)	210 × 16	35 × 35	50 × 50
Secant modulus at 5% strain (kN/m)	200	160	70
Material	High density polyethylene (HDPE)	High density polyethylene (HDPE)	Non-oriented polypropylene

**Fig. 2** Sequence of embankment model construction and testing. **a** Mixing of soft clay, **b** filling of geocells, **c** compacting the embankment, **d** test set-up

embankment and also controlled the heave of the soil adjacent to the embankment. Aspect ratio, which is the

ratio of height to diameter of the geocell, is an important factor that governs the deformations in the embankment.

Fig. 3 Variation of vertical deformations in an embankment supported on a geocell layer with different aspect ratios of geocells



The optimum value of aspect ratio for the test configurations and materials used in these model tests was found to be unity.

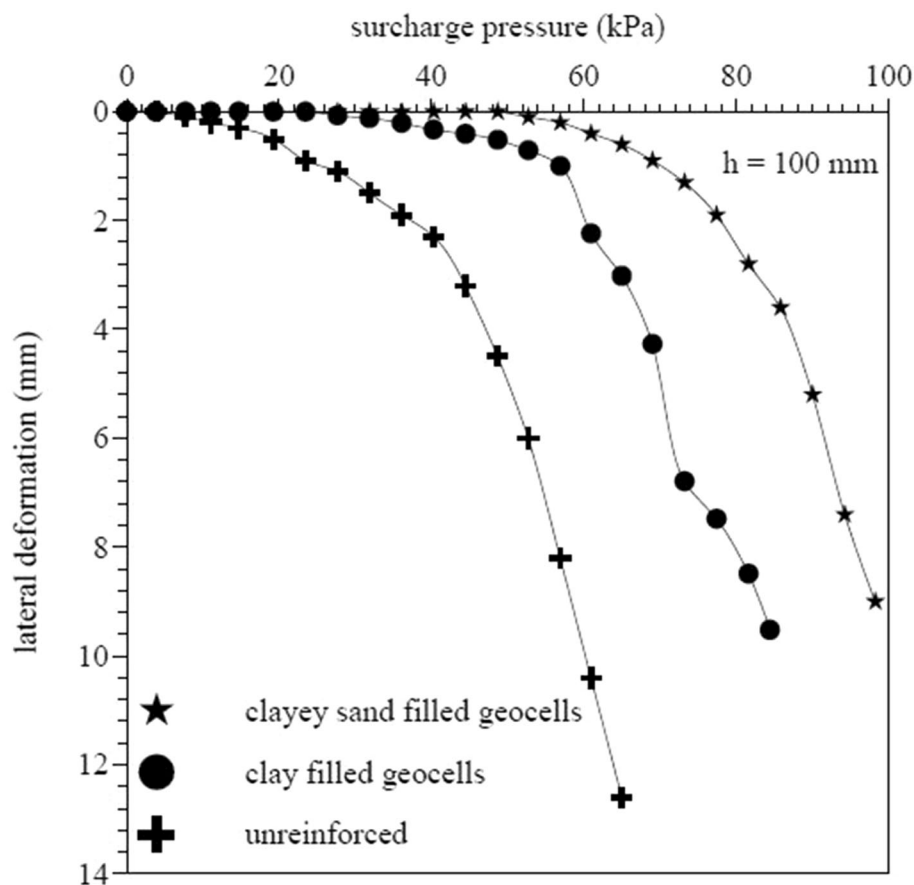
The geocell supported embankment with the cell aspect ratio of unity has settled three times less compared to an identical embankment constructed on the soft clay layer, without the geocell layer. When the performance of geocells made of uniaxial geogrid, biaxial geogrid and geonet is compared, geocells made of uniaxial geogrid performed better, because of their higher tensile stiffness.

Unreinforced embankment failed at a surcharge pressure of 50 kPa, whereas the embankments reinforced with geocells made up of uniaxial geogrid, biaxial geogrid and

geonet failed at surcharge pressures of 96 kPa, 75 kPa and 65 kPa, respectively, when the aspect ratio of cells was 0.44. The maximum vertical settlements recorded for the unreinforced embankment was 150 mm at 50 kPa and it reduced to 100 mm, 80 mm and 70 mm at the same surcharge pressure for embankments reinforced with geocells made of geonet, biaxial geogrid and uniaxial geogrid, respectively. The order of reduction is in the order of the tensile stiffness of the geocells.

Also, the economical benefits of geocells can be seen from Fig. 4, where the cells made of uniaxial geogrid were filled with the native clay material instead of clayey sand. Even with a clay infill, significant improvement in the

Fig. 4 Variation of lateral deformations in an embankment supported on a geocell layer filled with different soils



performance in terms of reduction in lateral deformation can be seen. The unreinforced embankment showed a load-carrying capacity of 50 kPa, whereas the reinforced embankments with clay and clayey sand showed load-bearing capacity of 65 kPa and 85 kPa, respectively, as seen in Fig. 4.

At a surcharge pressure of 50 kPa, the lateral deformation measured in the unreinforced embankment was 5 mm, whereas it reduced to 0.5 mm with the inclusion of clay-filled geocells. The embankment supported on geocells filled with clayey sand did not show any lateral deformations up to a surcharge pressure of 50 kPa. The embankment built directly on the soft clay bed has moved laterally by about 6 mm under a surcharge pressure of 50 kPa. However, the embankment supported on clay-filled geocell layer has deformed only by about 0.6 mm. The embankment supported on clayey-sand-filled geocells has not undergone any lateral deformations under 50 kPa.

Geocell-Faced Retaining Walls

Transportation geotechnical applications have retaining walls to serve functions like gradient change, slope protection and elevated corridors. Most of the gravity retaining walls are being replaced with reinforced soil walls, to provide flexibility and resistance to seismic loads. Geocell walls provide attractive and economical solutions for such scenarios, given the ease of their construction and their geometrically stable configuration. Unlike other types of mechanically stabilized soil retaining walls, geocell walls do not require any facing. The key design principle of a geocell retaining wall is to counteract the cyclic vehicular loads, wind loads and seismic loads through the additional friction and resisting moment generated at the base of the wall. Since geocell walls are built by stacking the layers of geocells, the entire width of the geocell layer acts as the reinforced fill and the driving forces from the weight of the retained backfill are counteracted by the gravitational forces exerted by the reinforced fill. The failure wedge shifts to much deeper into the fill, increasing the shear resistance under active and passive pressure conditions. The stacked geocells themselves act as the facing of the wall and if an offset is provided between different layers, grass and other

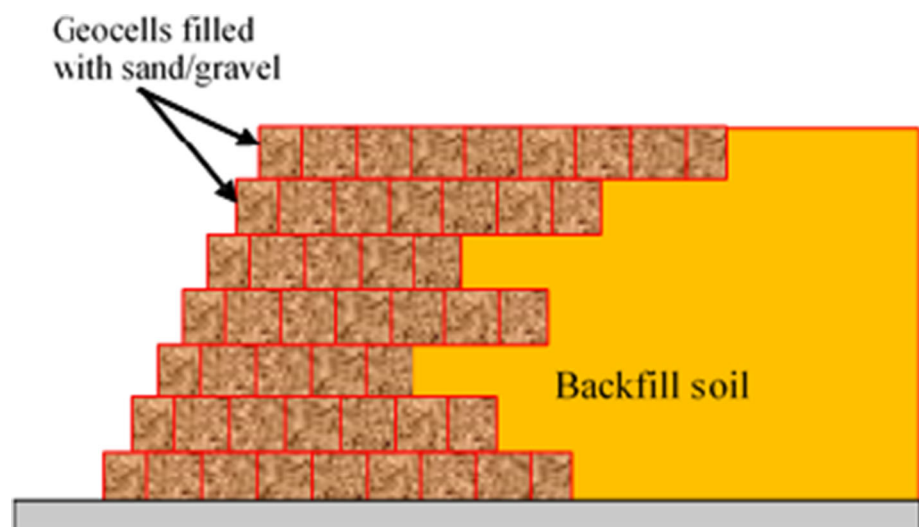
bio-stabilizing plants can be grown in cell pockets, which will further contribute to the stability of the wall [17]. The porous walls of the geocells restrict the development of pore pressures inside the fill, thus reducing the danger of wall collapse and liquefaction. These walls are extremely stable against seismic loads since the design provides flexibility and makes the entire structure ductile, allowing displacement adjustments between the layers, unlike full-height rigid-faced walls or gravity walls. Fig. 5 shows the schematic diagram of a commonly adopted geocell wall.

One of the important advantages of geocell walls is their resistance to earthquake shaking that comes from the wider facia, which is effective in resisting both sliding and overturning of the wall. To understand the response of geocell-faced walls to earthquake shaking, geocell-faced walls constructed in a laminar shear box were tested on a uni-directional shaking table. Low strength geonets were used to create the geocell facing. The sequence of steps followed for the construction of a geocell-faced wall inside the laminar shear box mounted on the uni-directional shaking table is shown in Fig. 6. Initially, the geocell layer of 100 mm height and 100 mm diameter is expanded to the required width of the box (0.5 m) and filled with aggregate of average size 10 mm and compacted. Backfill sand is then filled to the height of the geocell layer and compacted. Then, the next layer of geocells is placed above the first layer with an offset of 50 mm and filled with aggregates and compacted. This step is followed by the backfill sand filling up to the second layer. These steps are repeated till the full height of the geocell-faced wall (0.6 m) is reached. Displacements of the model walls were continuously monitored using ultrasonic displacement transducers, which can measure 20 displacement values within each second, with an accuracy of 1 μm . Also, these transducers

are not in contact with the models and hence they remain undisturbed during the model testing.

The model walls were shaken with different amplitudes and frequencies of shaking. It was observed that the geocell-faced walls stayed intact even after severe shaking conditions. For example, Fig. 7 shows the results from a set of simulated shaking studies, where the models were shaken to a frequency of 1 Hz, changing the amplitude of shaking between 0.2 and 0.3 g in tests S3A2F1 and S3A3F1, respectively. These values of acceleration amplitude represent moderate and severe seismic conditions. Deformation of geocell-faced walls at different elevations measured in tests with two different acceleration amplitudes is shown in Fig. 7a. For a moderate seismic shaking of 0.2 g amplitude, the wall deformed by a maximum amount of 4.2 mm and for severe seismic shaking of 0.3 g amplitude, the wall deformation was 5 mm. For an acceleration amplitude of 0.2 g, the deformation at the top of the retaining wall was found to be 4.2 mm, whereas for an acceleration amplitude of 0.3 g, the horizontal displacement was 5 mm. Another set of model tests were carried out at a shaking frequency of 2 Hz and the deformations corresponding to 0.2 g and 0.3 g acceleration amplitudes from tests S3A2F2 and S3A3F2, respectively, are presented in Fig. 7b. This situation corresponds to much severe shaking of the wall and for this condition, the wall displaced by a maximum about of 4.8 mm at an amplitude of 0.2 g and 5.5 mm at an amplitude of 0.3 g and for a frequency of 2 Hz, as shown in Fig. 7b, the values were 4.8 mm and 5.5 mm, respectively. However, the wall did not fail even under such severe seismic shaking conditions, proving that the geocell-faced walls have extremely high resistance to earthquake shaking.

Fig. 5 A typical geocell-faced retaining wall



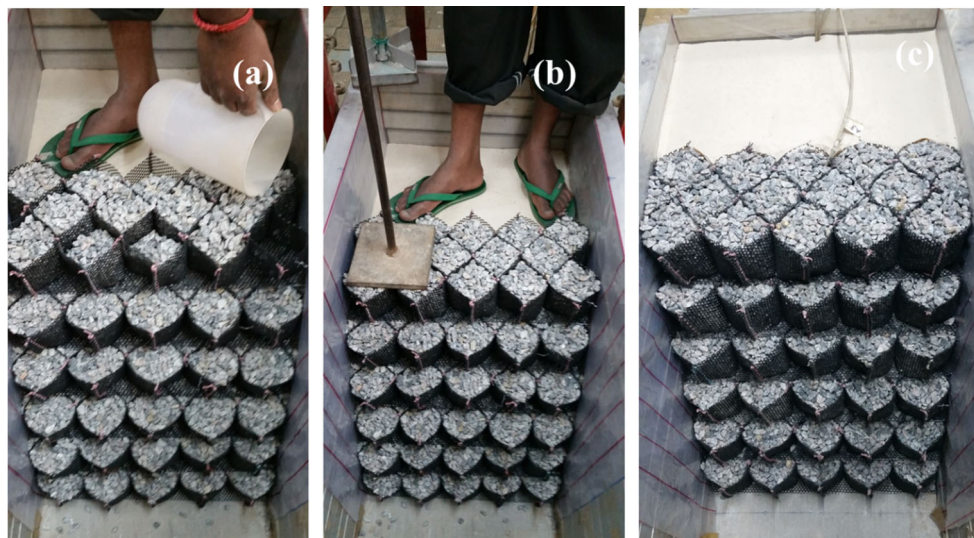


Fig. 6 Steps followed for constructing the geocell-faced walls. **a** Filling aggregate in cells, **b** compacting infill, **c** finished wall

Geocell Reinforced Unpaved Roads

Geocells perform multiple functions when used to reinforce unpaved roads. Apart from providing tensile and shear resistance to the road, their network can act as a separator between the soft subgrade and sub-base/base courses, limiting the mud-pumping and layer mixing. By providing a layer of geocells in the road section, the thickness of the aggregate layer can be significantly reduced with additional advantage of increased strength and resilience. Being a porous inclusion, geocells also allow free drainage between the layers and restrict the development of excess pore water pressures within the road sections.

To understand the beneficial effects of geocells in unpaved roads, laboratory plate load tests were carried out on model sections with geocell reinforcement. In a steel test tank, a clay subgrade is created using low plastic clay by compacting it to a unit weight of 18 kN/m^3 at its optimum moisture content of 15%. Under these conditions, the CBR value of the subgrade clay is 19%. Literature suggests that best benefits of geocell reinforcement are obtained when the CBR value of the subgrade is less than 10% [18]. In the present study, the strength of the subgrade is high, representing a stiffer subgrade. Stiffer subgrade was selected to facilitate identical model preparations in lesser time. With weaker subgrades, the beneficial effects will be much higher, due to additional beam effect and membrane effect generated between the weaker subgrade and the high strength polymeric reinforcement. Repeated load type plate-load tests were carried out on the model road sections built using aggregate of average size 10 mm above the clay

layer. This size corresponds to the least size of Grading 3 of granular sub-base design, specified for rural roads by the Ministry of Rural Development, India, as per the document published by the Indian Roads Congress (IRC), New Delhi in 2014. Commercial geocells with honeycomb shape and porous walls, supplied by Strata geosystems were used to reinforce the aggregate base layer. Height of the geocell layer was varied in different model tests, starting from 25 mm to 150 mm, in increments of 25 mm. The test sections have square dimensions of 0.75 m sides in plan and 0.62 m height. Figure 8 shows the schematic representation of the model test set-up.

Once the model was set up, the subgrade was subjected to repeated loading conditions by applying a constant pressure of 300 kPa on the circular plate resting on the subgrade, using a hydraulic jack. Hence, the repeated loading mechanism represents stress-controlled testing, where the pressure was applied repeatedly for 100 cycles on the model sections. Dial gauges mounted on the plate recorded the vertical displacements. 5 kPa of seating pressure was constantly applied while unloading, to ensure the contact between the plate and the subgrade. Each loading and unloading cycle took about 3 minutes. Reduction in the vertical deformations of the road sections with the inclusion of geocell layers of different heights is shown in Fig. 9. The plot shows diminishing benefits beyond a cell height of 75 mm, suggesting possible buckling that can happen in cell walls with further increase in height. The maximum reduction in vertical deformations was observed to be about 70%. In the repeated load testing, vertical deformations are categorized into elastic and plastic settlements. Plastic settlements are detrimental to

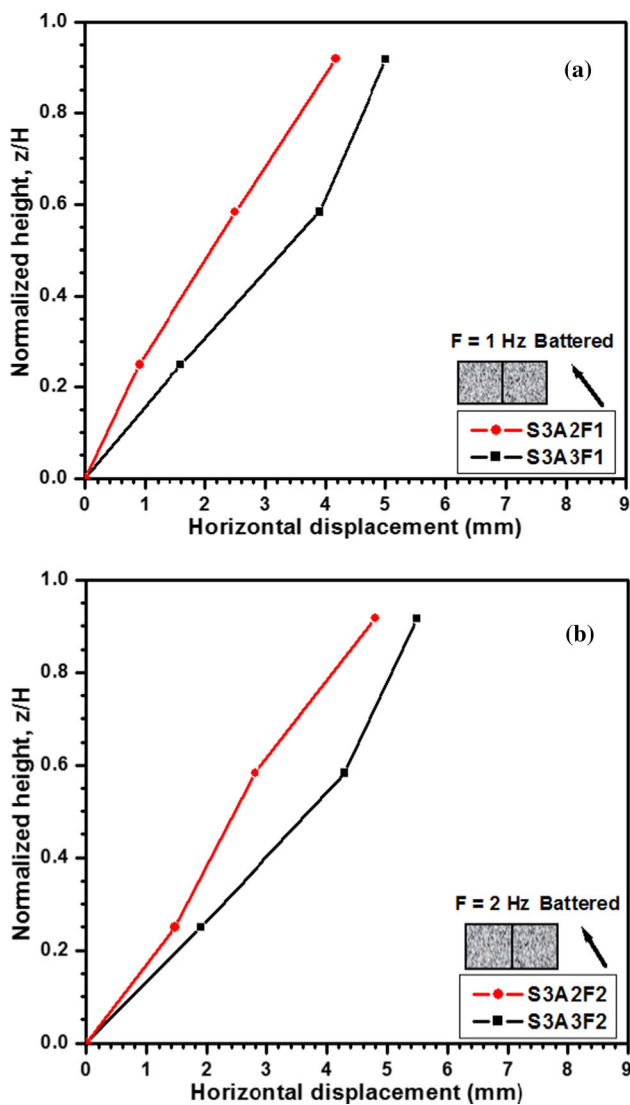


Fig. 7 Facing deformations in geocell walls for moderate and high seismic conditions. a 1 Hz frequency, b 3 Hz frequency

the performance of the roads since they represent the fraction of settlements that will be permanent, unlike elastic settlements. For the benefit of road service and maintenance, plastic settlements should be less. Comparison of plastic settlements accumulated in unreinforced road section and different geocell reinforced road sections is shown in Fig. 10. While the plastic settlement in unreinforced road section is about 110 mm at the end of 100 cycles of load, geocell reinforced section with 75 mm cell height could bring down the plastic settlements to less than 50 mm. Reduction in stiffness of the geocell with increase in height is a factor that should be considered in the design since geocells with height beyond 75 mm have shown comparatively lesser benefits.

To demonstrate the effectiveness of geocells for unpaved roads in a field set-up, small-scale field tests were

carried out on the Indian Institute of Science campus. An unpaved road section of 2 m length and 1 m width was chosen for these tests. The natural sandy soil subgrade of the campus has a CBR value of around 20%. The native soil was ploughed to a depth of 0.5 m and mixed with excessive amount of water and left for a day after mixing. The CBR value of the prepared test bed was measured as 1%. Aggregate of average size of 12 mm was used as the base course. Geocells were formed using a planar biaxial geogrid having ultimate tensile strength of 40 kN/m. Height and pocket size of the geocell layer were kept as 100 mm, which means that the aspect ratio of geocells was unity. The formation of a single geocell layer of 2 m² plan area consumed a planar geogrid of 5.85m² area. A geotextile layer having ultimate tensile strength of 55 kN/m was used as a basal layer for the geocells. In a different series of tests, only the planar geotextile and only the planar biaxial geogrid were used as reinforcement, instead of geocells. The cell pockets were filled with aggregate to a unit weight of 13 kN/m³. Prepared subgrade with geocell layer above the basal layer is shown in Fig. 11.

A cover layer of 50 mm thickness is created above the geocell layer to facilitate smooth movement of vehicles by mixing the native soil with 10% water by weight. After the cover layer is finished, the road section is subjected to moving vehicular loading. A Honda Activa two-wheeler motor vehicle of 100 kg weight was used for this test. The weight of the rider was 55 kg. The vehicle was driven along the central line of the road section at a uniform speed of 20 kmph. The vehicle generates a contact stress of about 8.5 kPa under both the wheels. This exercise was repeated 250 times and each time, the vehicle was allowed to move on the test bed at the same speed in the forward direction only, simulating on-way traffic. The entire road section was divided into equal area grids and the displacements were measured at the grid junctions at Sections 1, 2 and 3 as shown in Fig. 12 after every 50 passes of the vehicle. These displacements were used to calculate the rut depths. The rut depths were measured at marked grid points after every 20 passes until 250 passes were completed.

As observed from the rut depth measurements along the three transverse sections of the road shown in Fig. 12, geocell layer is very effective in controlling the rut depth. Unreinforced road section (UR) developed deeper ruts and the vehicle started skidding on it within 20 passes of the vehicle. However, the road section with geocell reinforcement (GC5.85) developed less deeper ruts and the vehicle passage was smooth till 250 passes. Between geotextile (GT) and geogrid (BG), geotextile performed better since the function of separation controlled the mixing of softer subgrade soil into the aggregate.

Fig. 8 Schematic diagram of the model set-up for repeated load tests on unpaved roads

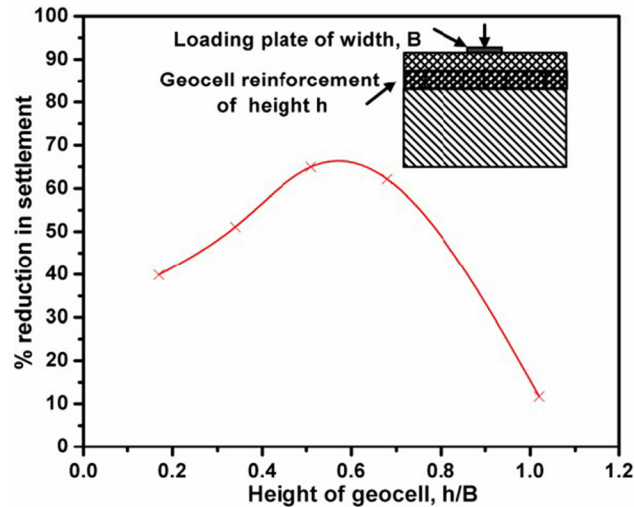
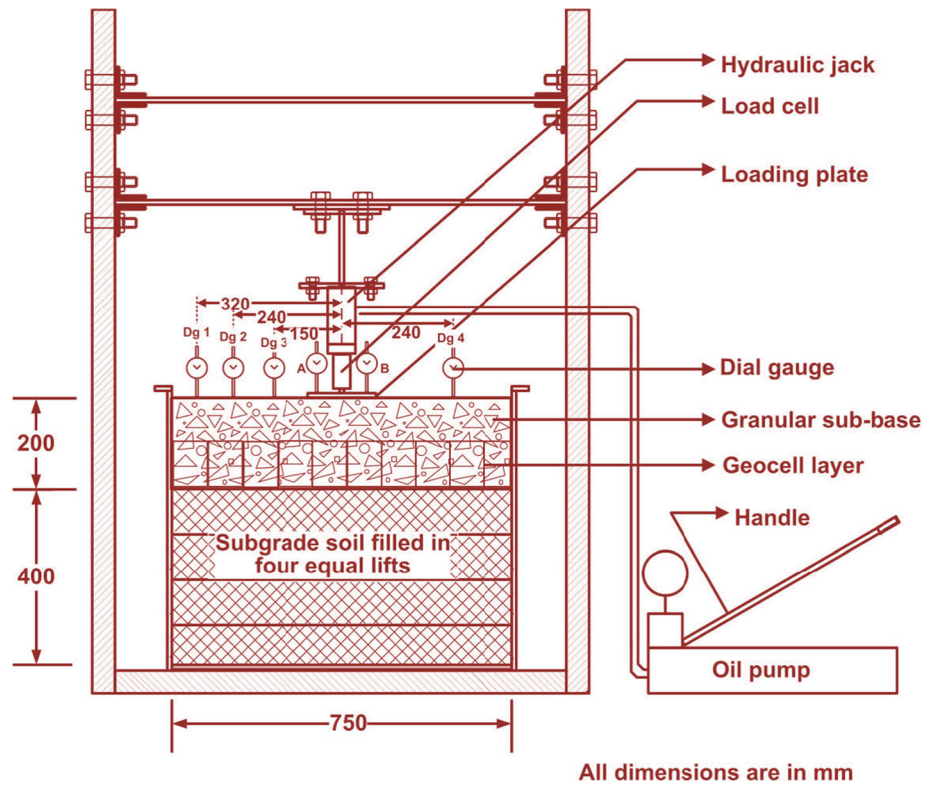


Fig. 9 Performance of geocell layer in reducing settlements in roads

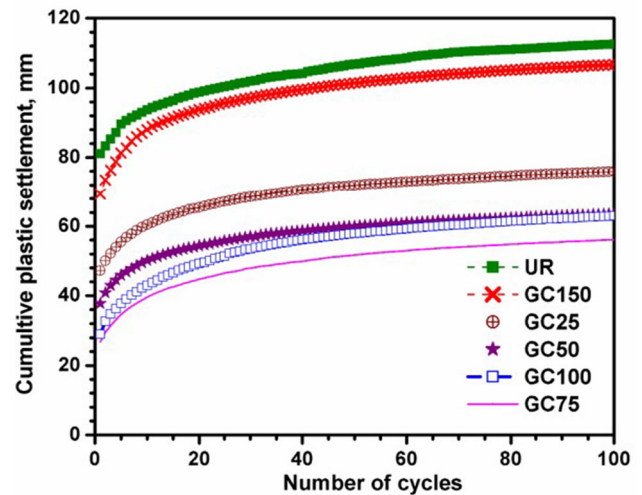


Fig. 10 Plastic settlements of road sections with geocell reinforcement

Summary

As demonstrated through various laboratory and field studies in this paper, geocells have multiple roles in transportation geotechnical applications. Their role in supporting road embankments on weak subgrade soils, soil retaining for cutting and filling operations related to road creation and widening, creating strong and sustainable

roads that can sustain many cycles of wheel loads is explained through model tests and field tests. In case of embankment support, the major function of geocells is spreading the load over wider area to reduce the zone of load influence so that the settlements of the soft layer can be reduced and lateral squeezing out of soil layer sandwiched between the embankment and the rigid base is

Fig. 11 Geocell layer prepared at the site



controlled. In case of geocell-faced retaining walls, geocells play the role of soil retention, as they replace the full-height rigid facing or panel facing, which are commonly used in reinforced retaining walls. Geocells in the retaining wall also provide lateral confinement effect to control wall deformations, flexibility between layers to adjust the deformations between the layers, particularly during seismic events and act as wave impeding layers, to control the acceleration amplifications at the crest. In case of road reinforcement, the mechanism of geocells is reduction of vertical and lateral deformations due to all-round confinement effect, providing a rigid mat to the wheel loads due to the beam effect of geocells and uniform and wider distribution of wheel loads to provide uniform deformations and better rideability. The laboratory repeated load tests and field tests with vehicular loads demonstrated the superior performance of geocell reinforced roads compared to unreinforced and planar geosynthetic reinforced roads, by sustaining much higher number of load cycles without getting damaged. In all these applications, though the mechanisms of interaction of geocells with soils are different, the main benefits of geocells are derived from the honeycomb-shaped interconnected hollow structure of geocells, which provides all-round confinement, overall stability and stiffness, with optimal usage of polymeric material. There is a greater scope for these materials in several other applications, including high speed rail

corridor abutments, providing erosion control and tsunami barrier systems that can sustain severe wave loads, creating flood protection barriers and blast proof roads and walls.

Conclusions

Beneficial effects of geocells in various transportation geotechnical applications are highlighted in this paper through various laboratory model experiments and small-scale field studies. Road embankments constructed on soft clay foundations supported on a geocell layer, retaining walls built with geocell facing and unpaved roads stabilized with a geocell layer were tested under static, cyclic and seismic shaking conditions. These studies brought out the advantages of using geocells for reinforcing soils for various transportation engineering applications. With the support from the geocell layer, embankments settled less and the slope deformations were completely arrested. Under repeated loading conditions, the geocell reinforced unpaved road sections showed lesser plastic settlements and higher load-bearing capacity compared to unreinforced road sections. Field tests with soft subgrades stabilized with geocell layer showed that the rut depth decreased substantially with the geocell reinforcement. Geocell reinforced road sections could sustain many vehicle passes without failure. Seismic load studies on geocell-faced walls

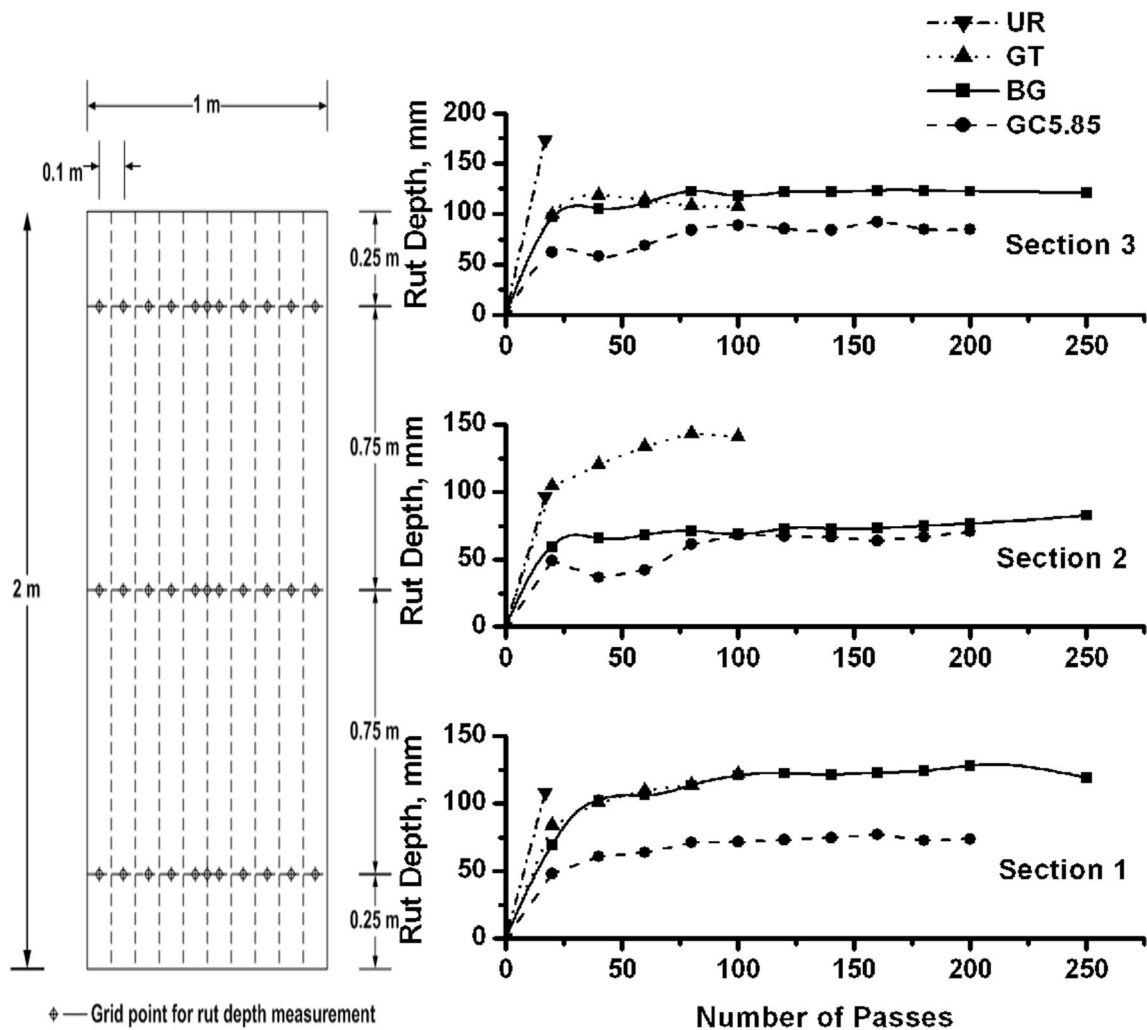


Fig. 12 Effectiveness of geocell layer in controlling the rut depths

highlighted their effectiveness under most severe earthquake conditions.

References

- Webster SL, Alford SJ (1978) Investigation of construction concepts for pavements across soft ground. Technical report S-78-6, United States Army Corps of Engineers, Waterways Experiment Station, Mississippi, USA
- Rea C, Mitchell JK (1978) Sand reinforcement using paper grid cells, Preprint 3130, ASCE spring convention and exhibit, Pittsburgh, PA, pp 644–663
- Pokharel SK, Martin I, Norouzi M, Breault M (2015) Validation of geocell design for unpaved roads, Geosynthetics Feb 15–18, 2015, Portland, OR, USA
- Geocell Systems (2012) Introducing the rapid deployment flood wall. <http://www.geocellsystems.com/>. Retrieved on 12th November 2020
- PRS Geotechnologies (2009) Steep reinforced retaining walls meet complex requirements. <https://www.prs-med.com/casestudies/15m-retaining-wall-residential-buildings/>. Retrieved on 12th November 2020
- Bagli S (2012) Geocells: the way forward with the three dimensional innovation. <http://www.stratindia.com/img/media/GeoInfra-Geocells-Final.pdf>. Retrieved on 12th November 2020
- Han J, Pokharel SK, Yang X, Manandhar C, Leshchinsky D, Halahmi I, Parsons RL (2011) Performance of geocell-reinforced RAP bases over weak subgrade under full scale moving wheel loads. *ASCE J Mater Civ Eng* 23(11):1525–1535
- Bathurst RJ, Karpurapu R (1993) Large scale triaxial tests on geocell reinforced granular soils. *Geotech Test J* 16(3):296–303
- Rajagopal K, Krishnaswamy NR, Latha GM (1999) Behavior of sand confined in single and multiple geocells. *Geotext Geomembr* 17:171–184
- Krishnaswamy NR, Rajagopal K, Latha GM (2000) Model studies on geocell supported embankments constructed over a soft clay foundation. *Geotech Test J ASTM* 23(2):45–54
- Latha GM, Nair AM, Hemalatha MS (2010) Performance of geosynthetics in unpaved roads. *Int J Geotech Eng* 4(2):151–164
- Nair AM, Latha GM (2016) Repeated load tests on geosynthetic reinforced unpaved road sections. *Geomech Geoen* 11(2):95–103

13. Latha GM, Manju GS (2016) Seismic response of geocell retaining walls through shaking table tests. *Int J Geosynth Ground Eng* 2(7):1–15
14. Thakur JK, Han J, Leshchinsky D, Halahmi I, Parsons RL (2011) Creep deformation of unreinforced and geocell-reinforced recycled asphalt pavements. In: Han J, Alzamora DE (eds) *Proceedings of geo-frontiers 2011: advances in geotechnical engineering*, ASCE, New York, pp 4723–4732
15. Leshchinsky B (2011) Enhancing ballast performance using geocell confinement. In: Han J, Alzamora DE (eds) *Proceedings of geo-frontiers 2011: advances in geotechnical engineering*, ASCE, New York, pp 4693–4072
16. Saride S, Rayabarapu VK (2020) Design of geocell reinforced pavement bases. In Sitharam TG, Amarnath MH, Kolathayar S (eds) *Geocells*, Springer Transactions in Civil and Environmental Engineering, Springer Nature, Switzerland AG, pp 225–255
17. Han J, Guo J (2017) Geosynthetics used to stabilize vegetated surfaces for environmental sustainability in civil engineering. *Front Struct Civ Eng* 11(1):56–65
18. Alimohammadi H, Zheng J, Schaefer VR, Seikmeier J, Velasquez R (2021) Evaluation of geogrid reinforcement of flexible pavement performance: a review of large-scale laboratory studies. *Transp Geotech* 27:100471

Publisher's Note Springer Nature remains neutral with regard to jurisdictional claims in published maps and institutional affiliations.